Remote Guidance Method of Unmanned Aerial Vehicle Based on Multi-sensors

Xiao Liang
School of Automation
Shenyang Aerospace University
Shenyang, China
connyzone@126.com

Guodong Chen
School of Automation
Shenyang Aerospace University
Shenyang, China
cgd1128@163.com

Shirou Zhao
School of Automation
Shenyang Aerospace University
Shenyang, China
zsrou2018@163.com

Guangbo Tong
School of Automation
Shenyang Aerospace University
Shenyang, China
694859836@qq.com

Linping Jiang
School of Automation
Shenyang Aerospace University
Shenyang, China
1536118384@qq.com

Wei Zhang
School of Mechanical Engineering
Nanjing University of Science and Technology
Nanjing, China
337456998@qq.com

***Abstract*—Aiming at the problem that single sensor cannot balance the distance of guidance and accuracy, the paper proposes a remote guidance method for UAV (Unmanned Aerial Vehicle) based on multi-sensors. This paper first introduces the remote guidance and autonomous landing task. Then the hardware and control method are designed. The landing process is divided into two stages: the long-range and close-range. In order to take advantage of the characteristics of different sensors, GPS/IMU (Inertial Measurement Unit) hybrid guidance is used for long-range stage and visual guidance is used for close-range stage. The positioning and guidance method are also introduced in detail. In close- range stage, according to the requirements of accurate landing on mobile UGV (Unmanned Ground Vehicle), the vision guidance method based on Apriltag is proposed and the calculation of UAV attitude and relative distance is completed. EKF (Extended Kalman Filter) is used as the multi-sensors fusion method. Finally, the method is applied to a quadrotor and Mecanum UGV and an outdoor experiment is realized and analyzed. The experimental results show that the accuracy and real-time ability of the proposed method meet the requirements of UAV's landing on a mobile UGV from a long distance.**

Keywords—Autonomous landing of mobile platform; guidance of long-range and close-range; Multi-sensors; EKF; Apriltag

I. INTRODUCTION

With the rapid development of science and technology, the applications of aerial robots (also known as unmanned aerial vehicles, UAV) and ground robots (unmanned ground vehicle, UGV) are getting more and more attention form researchers all over the world. UAV can quickly detect broader areas, but its endurance is limited. Although UGV moves at a slower speed, its endurance is better basing on the advantage of moving on ground. Therefore, the carrier-based aircraft of UGV has attracted the attention of many researchers. In carrier-based aircraft of UGV, the remote guidance of UAV's landing is an important basis for the coordination of UAV/UGV heterogeneous system.

The key of guidance based on carrier-based aircraft of UGV is positioning and the accuracy of positioning will directly affect the quality of guidance. At present, the main positioning methods include GPS positioning [1], base station positioning [2], WiFi positioning [3], Bluetooth positioning [4], image positioning [5] and so on. However, there are some common problems of a single sensor in positioning. Generally, sensors in a long positioning distance usually have low positioning accuracy and its accuracy will increase with the decrease of measurement distance. Sofia et al [6] proposed a robot positioning system with multi-sensor fusion. Li et al [7] proposed a vehicle positioning system with multi-sensor fusion. From the simulation and experiment, both of them achieve a higher precision positioning. With the improvement of positioning accuracy, the guidance technology has also developed rapidly. Guidance technology has been widely used in air refueling, landing of carrier aircraft, interception of missile and so on. Hu et al [8] use Kalman filter to fuse GPS and visual information and obtain the relative position of two UAVs. In their research, an improved linear quadratic regulator controls the UAV to make precise docking. Tang et al [9] realizes the precise positioning of UAV based on the information of IMU, GPS and vision sensor. They calculate the exact relative position by Kalman filter and finally realize the autonomous landing of UAV with high accuracy. Both of the above methods can achieve precise guidance, but they are only verified in simulation. Wenzel et al [10] use IR camera to realize UAV landing. The landing effect is better without direct sunlight. Lee et al [11] realize the patrol of UAV and the tracking and landing is based on vision. Since their methods are all visual guidance, they are not suitable for long-distance guidance. Araar et al [12] studies the autonomous landing of quadrotor on static and dynamic targets and designs a new landing platform which can make pose estimation. They use extended Kalman filter and extended visual solution data for fusion which will reduce the possibility of losing target. About UAV's landing on a high-speed moving vehicles, Borowczyk et al [13] combines IMU, GPS and visual measurements to provide their system with position. In their research, velocity and gravity-compensated acceleration data are directly expressed in the global NED (North-East-Down) frame. They place a mobile phone on the landing pad, which transmits its GPS and IMU data to UAV by WiFi. Kalman filter is adopted to fuse sensor data to estimate the position of quadrotor. However, because of the limited transmission distance by WiFi, the system is not suitable for long-range guidance. In summary, most of the above methods are only suitable for the case of tracking and landing in a short distance. If UAV approaches and lands on UGV from a long distance, the method of guidance needs a novel scheme.

Aiming at the task of UAV's approaching and landing on a mobile UGV platform from a long distance, the paper proposes a guidance method based on multi-sensors. By the

This work is supported by National Natural Science Foundation of China under Grant 61973222, 61503255 and 61906125, Aeronautical Science Foundation of China under Grant 2016ZC54011, Natural Science Foundation of Liaoning Province under Grant 2015020063.

978-1-7281-3792-6/19/$31.00 ©2019 IEEE

combination of GPS/IMU and machine vision, the method can balance the relationship between guidance distance and accuracy. Finally, the proposed method is verified by physical experiments and the task of UAV's landing on a moving UGV from a long distance is realized.

II. UAV Modeling and Control

A. Platform of Modeling

QStudioRP simulation platform is developed by Quanser in Canada. It is an integrated open platform for the development, design, simulation and test of quadrotor [14]. The hardware system mainly includes motor/rotor, encoder (sensor), power modules and quadrotor, which are shown in Fig. 1 and listed in Table 1.

Fig. 1. Main structure of QStudioRP simulation platform.

TABLE I. Device specifications

Name	Value
Helicopter body mass	$1.39kg$
Helicopter body length	$48cm$
Base dimensions	$17.5cm \times 17.5cm$
Encoder resolution	$8192\,counts/rev$
Pitch angle range	$75(\pm 37.5\deg)$
Yaw angle range	$360\deg$
Propeller diameter	$20.3cm$
Propeller pitch	$15.2cm$
Motor armature resistance	0.83Ω
Motor current-torque constant	$0.0182\,N\cdot m/A$

B. System Description

According to definition [15], the quadrotor is motivated by four motors and has three attitudes, which is yaw, pith and roll. Define $v=(x,y,z,\psi,\theta,\phi)\in R^6$ where $\xi=(x,y,z)\in R^3$ presents the position and $\eta=(\psi,\theta,\phi)\in R^3$ respectively denote yaw, pitch and roll angle. Then we can get that the kinetic energy of motion $T_{trans}=1/2m\xi^T\xi$ and the kinetic energy of rotation $T_{rot}=1/2m\eta^T\eta$, where m represents the mass of airframe. By using Lagrange method, the dynamic model of quadrotor can be presented as [16]:

$$\begin{cases}\ddot{\psi}=\dfrac{K_{tn}}{J_\psi}l(V_f+V_b)+\dfrac{K_{tc}}{J_\psi}l(V_r+V_l)\\ \ddot{\theta}=\dfrac{K_{tn}}{J_\theta}l(V_f-V_b)\\ \ddot{\phi}=\dfrac{K_{tc}}{J_\phi}l(V_r-V_l)\end{cases}\tag{1}$$

Here, K_{tn} and K_{tc} are respectively counter rotation propeller torque-thrust constant and normal rotation propeller torque-thrust constant, J_θ is equivalent moment of inertia about the pitch axis, J_ϕ is equivalent moment of inertia about the roll axis, J_ψ is equivalent moment of inertia about the yaw axis. V_f, V_b, V_r, V_l respectively represent the front, back, right and left motor's voltage.

C. Controller based on Linear Quadratic Regulator (LQR)

Define the state vector $x(t)=[\psi,\theta,\phi,\dot{\psi},\dot{\theta},\dot{\phi}]\in R^n$, output vector $y(t)=[\psi,\theta,\phi]\in R^q$, input vector $u(t)=[V_f,V_b,V_r,V_l]^T$. After linearization, the state equation of attitude channel is:

$$\begin{cases}\dot{x}_a(t)=A_a x_a(t)+B_a u_a(t)\\ y_a(t)=C_a x_a(t)\end{cases}\tag{2}$$

According to the theory of Linear Quadratic Regulator (LQR), the controller is:

$$u_a(t)=-L_a x_a(t)+L_{ra}h_a(t)\tag{3}$$

where L_a and L_{ra} is feedback gain matrix and feedforward gain matrix, respectively. h_a is input command. Choose the performance indicator is:

$$\begin{aligned}J=&\frac{1}{2}e_a{}^T(t_f)Se_a(t_f)\\&+\frac{1}{2}\int_{t_0}^{t_f}[e_a{}^T(t)V(t)e_a(t)+u_a{}^T(t)R(t)u_a(t)]dt\end{aligned}\tag{4}$$

In (4), $e_a=h_a-y_a$. S, $V(t)$, $R(t)$ is respectively the weighting matrix of $e_a(t_f)$, $e_a(t)$, $u_a(t)$. When performance indicator J reaches its minimum, there is:

$$\begin{cases}L_a=R^{-1}B_a{}^T\bar{P}\\ L_{ra}=R^{-1}B_a{}^T[\bar{P}B_aR^{-1}B_a{}^T-A_a{}^T]^{-1}C_a{}^TV\end{cases}\tag{5}$$

where $\bar{P}$ is the solution of Riccati equation, and V and R is diagonal matrix. According to (2) and (5), the closed-loop control system based on LQR is:

$$\begin{cases}\dot{x}_a=(\bar{A}_a-\bar{B}_a\bar{L}_a)x_a+\bar{B}_a\bar{L}_{ra}h_a\\ y_a=\bar{C}_a x_a\end{cases}\tag{6}$$

III. Design and Implementation of UAV

A. Construction of UAV Hardware System

The UAV uses a high-strength and lightweight carbon braze as a frame and a Pixhawk as the flight controller (Fig. 2). The STM32 controller generates PWM to SBUS Encoder. An OpenMV camera is connected to the STM32 controller. GPS is connected to the flight control. A wireless data transmission station is used for communication between UAV and UGV.

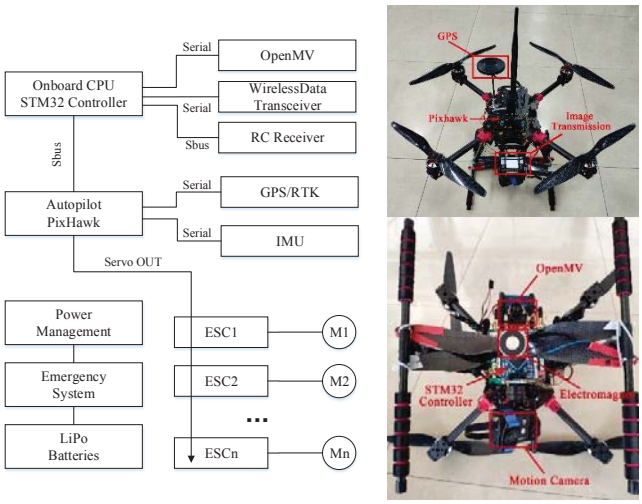

(a) Hardware structure of UAV (b) Physical photo of UAV

Fig. 2. UAV used in this research.

As shown in Fig. 2(b), UAV is equipped with two cameras. The motion camera is used to capture the image below the UAV and wirelessly transmit the image to the user for monitoring the area under the UAV. OpenMV camera is used to identify Apriltag [17] and is an image sensor for guidance when UAV and UGV are close. OpenMV is not good at wireless transmission, so the scheme of dual cameras is adopted. Since they are installed in different locations, the two images are also different.

B. Analog RC based on SBUS Protocol

In order to maintain the original stability of UAV and reduce the workload of developing flight control, the paper proposes an analog remote control method based on the SBUS protocol. The method uses a signal generation device to simulate the remote control signals to control UAV. A Pixhawk flight controller is used in UAV and connected to a signal translator (Fig. 3).

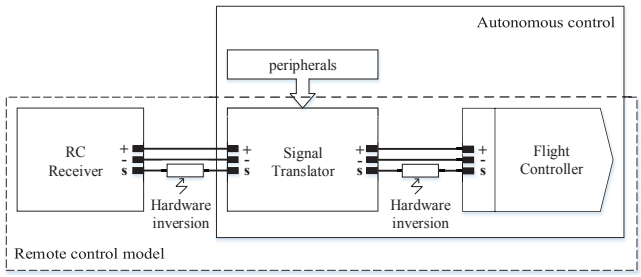

Fig. 3. Structure diagram of quadrotor control system.

The UAV has three flight modes: manual RC mode, automatic flight mode and emergency stop mode.

In manual RC mode, the receiver receives remote control data in real time and sends it to the signal translator through SBUS protocol. The data from remote controller is passed to flight controller by signal translator without any processing.

In automatic flight mode, the controller calculates the inputs for four motors first and then encodes and transmits these signals to achieve the purpose of automatic flight.

In emergency stop Mode, the signal translator immediately sets the values of all channels to middle, then encodes and sends them to achieve the purpose of UAV fixed-point hovering and ensure flight safety.

IV. Remote Guidance Method Based on Multi-sensors

There are many methods about positioning and guidance at present. However, the common problems are that the accuracy will decrease with the increase of measurement distance. The scheme of remote guidance and precise autonomous landing in this paper are shown in Fig. 4.

- The aim of long-range stage is to guide UAV to approach UGV.
- The aim of close-range stage is to prepare for landing. It is necessary to maintain the attitude of UAV.

The positioning and guidance methods of each stage are: GPS and IMU (Inertial Measurement Unit) are used for long-range stage and visual positioning is used for close-range stage. At last, EKF is used to fuse the data in order to achieve accurate positioning and guidance of UAV.

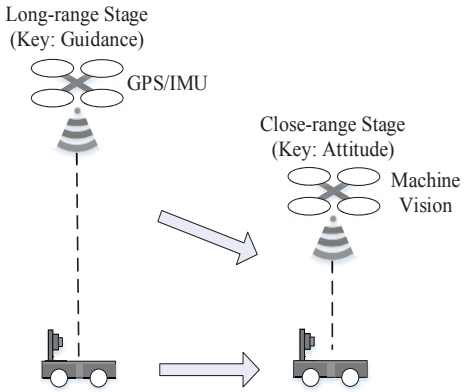

Fig. 4. Scheme of remote guidance and precise autonomous landing.

A. Guidance based on GPS in Long-range Stage

In this process, UAV is far away from UGV and the purpose is to quickly shorten the distance between UAV and UGV. So accuracy is not a major problem in this stage and GPS positioning method is adopted in this stage. In order to obtain the relative position between UAV and UGV, GPS is installed on UAV and UGV respectively. The Communication in long-range stage is shown in Fig. 5.

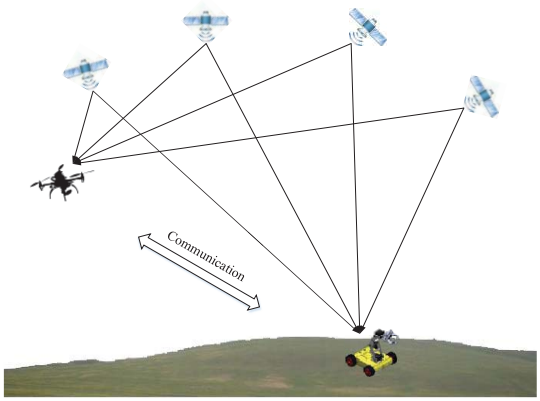

Fig. 5. Communication in long-range stage with GPS.

After obtaining their respective latitude and longitude, the UAV can be guided to the vicinity of UGV. UGV sends

its heading, longitude, latitude, and average speed V_G to UAV in real time. UAV calculates the distance D and angle q between UAV and UGV according to the above information. On the premise that the velocity V_A of UAV is known, the process of guidance in long-range stage is shown in Fig. 6. Here, T represents flight time.

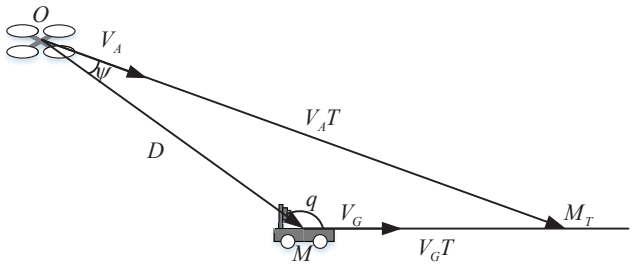

Fig. 6. Process of guidance in long-range stage.

Using pre-collision point guidance method, the guidance process can be described as:

$$V_G \sin q = V_A \sin \psi \tag{7}$$

$$\psi = \arcsin(\frac{V_G}{V_A} \sin q) \tag{8}$$

After angle ψ is obtained, UAV can calculate the velocity components on the roll and pitch axis according to its own heading and send them to controller. Then UAV will fly to the direction of UGV.

B. Guidance based on Apriltag in Close-range Stage

Apriltag [18] is an improved visual positioning system based on ARToolkit [19] and ARTag [20]. It is a visual reference library [21] and widely used in robots and UAV positioning guide [22]. Apriltag uses a simple Quick Response Code (QR Code) which has only 4 to 12 bits data and it can be easily detected in a long range.

Apriltag not only can identify and track the target, but also can get the 3D pose of the target. As long as the camera resolution, focal length and the size of tag are known, the algorithm can identify the type, ID, distance and attitude of the tag.

1) Detection and Identification of Tags

The Tag is a quadrangle which is inner black and outer white, as shown in Fig. 7.

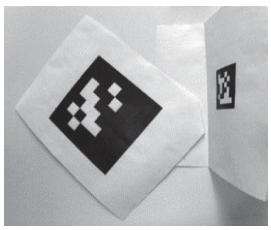

Fig. 7. Tags.

The tag detection algorithm begins by computing the gradient at every pixel, including their magnitudes (Fig. 8(a)) and direction (Fig. 8(b)). Using a graph-based method, pixels with similar gradient directions and magnitude are clustered into components (Fig. 8(c)). Weighted least square is used to fit these pixels of each component with a line segment (Fig. 8(d)). The direction of the line segment is determined by the gradient direction, so that segments are dark on the left, light on the right.

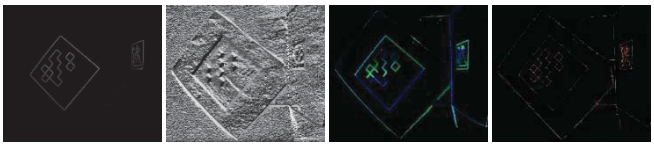

(a) (b) (c) (d)

Fig. 8. Detection process.

At this point, the Tag is transformed into a set of directed segments and then the sequence of segments of the quadrilateral is calculated basing on a recursive depth-first search with a depth of 4 [17].

2) Calculation of the Distance and Angle from Tag to OpenMV Camera

In homography transformation (one plane is mapped to another) and external parameter estimation, a 3×3 homography matrix (A conversion matrix when mapping, and the matrix is usually represented by H) needs to be calculated. It maps the coordinate system of the Tag to a 2D image coordinate system. Homography matrix is calculated by Direct Linear Transform (DLT) algorithm. The rotational component of E is represented as R_{ij} and the translational component is represented as T_k . s is scale factor, so:

$$H = \begin{bmatrix} h_{00} & h_{01} & h_{02} \\ h_{10} & h_{11} & h_{12} \\ h_{20} & h_{21} & h_{22} \end{bmatrix} = sPE = s \begin{bmatrix} f_x & 0 & 0 & 0 \\ 0 & f_y & 0 & 0 \\ 0 & 0 & 1 & 0 \end{bmatrix} \begin{bmatrix} R_{00} & R_{01} & T_x \\ R_{10} & R_{11} & T_y \\ R_{20} & R_{21} & T_z \\ 0 & 0 & 1 \end{bmatrix} \tag{9}$$

Here, h_{ij} is the element of homography matrix H . f_x and f_y are the focal length of camera respectively. It is not possible to solve E directly because P is not full rank. By calculating the right side of (6), each h_{ij} can be written into a set of equations:

$$\begin{cases} h_{00} = sR_{00}f_x \\ h_{01} = sR_{01}f_x \\ h_{02} = sT_xf_x \\ \cdots \end{cases} \tag{10}$$

The elements of R_{ij} and T_k can be easily determined. Each column of the rotation matrix must be a unit vector, so the limitation can be satisfied by different s . Since the rotation matrix has only two columns, s can be set as the geometric mean of the amplitude of matrix. Finally, by homography matrix, the relative coordinate system of tag is mapped to the coordinate system of image. Furthermore, the distance and angle from Tag to camera are finally obtained.

When OpenMV camera recognizes the Tag on the deck of UGV (as shown in Fig. 9), it automatically switches to the guidance of Apriltag.

Fig. 9. Deck of UGV.

C. Multi-sensors Fusion Method

The information of GPS and IMU is integrated in long-range stage. In short-range stage, the fusion results of GPS and IMU are fused with Apriltag again. In addition, there is no clear division between the two stages in guidance. After identifying the Tag by OpenMV camera, the process automatically switches to short-range stage.

For multi-sensors data fusion, EKF (Extended Kalman Filter) [23] is adopted. It uses discrete models with first-order approximation for nonlinear systems. EKF algorithm can compensate for each sensor's limitations. For nonlinear systems, a generic stochastic process can be described by a discrete system as follow.

$$\begin{cases} x_{k+1} = f(x_k, u_k, v_k) \\ y_{k+1} = h(x_k, w_k) \end{cases} \tag{11}$$

where x_k and y_k are the state vector and the observation vector, respectively. f and h are the state function and the observation function, respectively. u_k is the system input. v_k and w_k are the white Gaussian noise and the measurement noise with different covariance matrix Q_k and R_k, respectively. By linearized observation functions, the priori state estimate and the covariance matrix are given as

$$x_{k+1}^{-} = f(x_k^{+}, u_k, 0) \tag{12}$$

$$P_{k+1}^{-} = A_k P_k A_k^T + Q_k \tag{13}$$

where x_{k+1}^{-}, P_{k+1}^{-}, and x_k^{+} are the priori state at time k, the priori covariance at time $k+1$ and the posteriori state at time k, respectively. From the prediction (13) and (14), the posteriori estimate is as follow.

$$K_{k+1} = P_{k+1}^{-} H_k^T (H_k P_{k+1}^{-} H_k^T + R_k)^{-1} \tag{14}$$

$$x_{k+1}^{+} = x_{k+1}^{-} + K_{k+1}(z_{k+1} - H_k x_{k+1}^{-}) \tag{15}$$

$$P_{k+1}^{+} = (I - K_{k+1} H_k) P_{k+1}^{-} \tag{16}$$

where K_{k+1}, x_{k+1}^{+} and P_{k+1}^{+} are the Kalman gain, the posteriori estimate and the posteriori covariance, respectively. EKF is implemented using (11)-(16) to estimate the state and to complement different sensors.

V. Experiment and Analysis

In order to ensure the safety of the experiment, UAV in this experiment is always in the visible range. In other words, UAV is not far away from UGV at the beginning (as shown in Fig. 10(a)). In addition, in order to avoid the risk of rollover, an electromagnet is installed under the deck of UGV and used to hold UAV after its landing.

The picture in picture is the image returned by the motion camera. OpenMV is not good at wireless transmission, so the image of OpenMV is not provided here. Specially, the transmission of OpenMV will seriously affect the real-time performance and the serial port is not enough. Therefore, all of the images provided in this experiment are from motion camera.

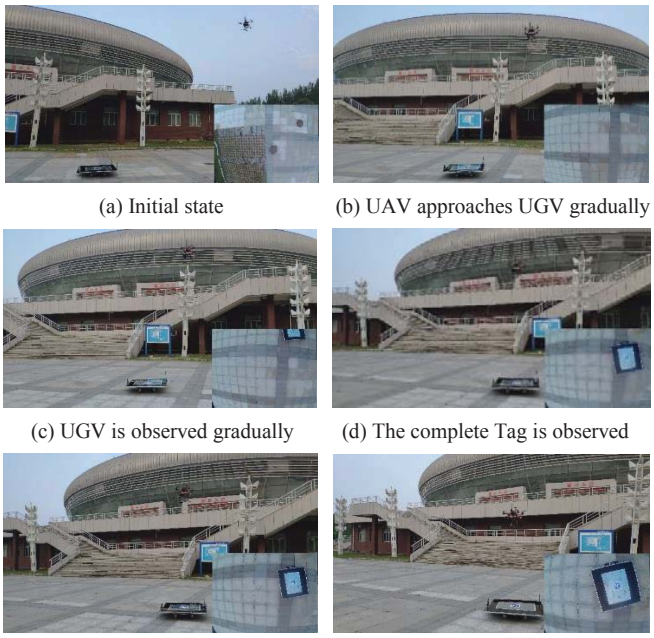

(a) Initial state (b) UAV approaches UGV gradually

(c) UGV is observed gradually (d) The complete Tag is observed

(e) UAV reduces its altitude (f) Transition between two stages

Fig. 10. Guidance based on GPS in long-range stage.

As shown in Fig. 10, the process can realize the rapid guidance of the UAV. When UAV reaches the place above UGV, it gradually decreases its altitude in order to allow OpenMV to recognize the Tag on UGV deck. Although a clear and complete Tag has appeared in Fig. 10(d)(e)(f), this is an image from motion camera. In fact, OpenMV has not recognize the Tag yet.

As the altitude of UAV gradually decreases, OpenMV recognizes the Tag (Fig. 11).

(a) Initial stage of close-range (b) UAV adjusts its attitude

Fig. 11. Guidance based on Apriltag in close-range stage.

Here, the switching process cannot be seen directly from these figures. However, by comparing Fig. 11 (a) and (b), the attitude of UAV changes obviously and the UAV and UGV have the same headings.

Then the UAV adjusts its attitude and position gradually. Finally, UAV lands on the deck of UGV (Fig. 12).

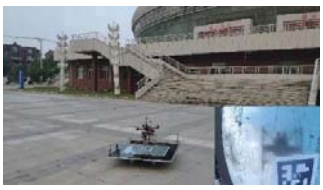

(a) UAV continues to reduce altitude

(b) Successful landing of UAV

Fig. 12. landing process of UAV.

In Fig. 12(a), the Tag is not directly below the UAV. The reason is that the installation location of the motion camera is different from OpenMV camera. In fact, the Tag is just below OpenMV camera. When UAV touches the UGV deck, the landing point of UAV changes due to inertia. After landing is stabilized, the electromagnet under the UAV will firmly hold UAV to the deck of UGV (Fig. 12 (b)).

VI. Conclusion

This paper first introduces remote guidance and autonomous landing tasks. Then, a QStudioRP simulation platform is used to model the quadrotor and the control method based on LVQ is proposed. In addition, in order to develop the quadrotor more efficiently and quickly, a multi-rotor autonomous flight control method based on SBUS protocol is proposed. Then the whole landing process is divided into two stages: long-range and short-range. GPS/IMU hybrid guidance is used for long-range stage and visual guidance is used for close-range stage. In multi-sensors fusion, EKF is introduced and adopted. The experiment results show that the proposed method can guide UAV approaches and lands on a moving UGV.

References

[1] Xingchuan Liu, Qingshan Man, Henghui Lu and Xiaokang Lin, "Wi-Fi/MARG/GPS integrated system for seamless mobile positioning," 2013 IEEE Wireless Communications and Networking Conference (WCNC), Shanghai, China, April 7-10, 2013.

[2] Matteo Ridolfi, Stef Vandermeeren, Jense Defraye and Heidi Steendam, "Experimental evaluation of UWB indoor positioning for sport postures," Sensors (Basel), vol. 18, no. 1, pp. 168-187, 2018.

[3] Chen Chen, Yan Chen, Yi Han, Hung-Quoc Lai and Feng Zhang, "Achieving centimeter-accuracy indoor localization on WiFi platforms: a multi-antenna approach," IEEE Internet of Things Journal, vol. 4, no. 1, pp. 122-134, 2017.

[4] Ling Pei, Jingbin Liu, Yuwei Chen, Ruizhi Chen and Liang Chen, "Evaluation of fingerprinting-based WiFi indoor localization coexisted with Bluetooth," The Journal of Global Positioning Systems, vol. 15, pp. 3-14, 2017.

[5] Guifeng Wu, Jie Zheng, Jiatong Bao and Shengquan Li, "Mobile robot location algorithm based on image processing technology," EURASIP Journal on Image and Video Processing, vol. 2018, pp. 107-114, 2018.

[6] Sofia Yousuf and Muhammad Bilal Kadri, "Robot localization in indoor and outdoor environments by multi-sensor fusion," 2018 14th International Conference on Emerging Technologies (ICET), Islamabad, Pakistan, November 21-22, 2018.

[7] Xu Li, Wei Chen, Chingyao Chan, Bin Li and Xianghui Song, "Multi-sensor fusion methodology for enhanced land vehicle positioning," Information Fusion, vol. 46, pp. 51-62, 2019.

[8] Hu Zhu, Suozhong Yuan and Qian Shen, "Vision/GPS-based docking control for the UAV Autonomous Aerial Refueling," 2016 IEEE Chinese Guidance, Navigation and Control Conference (CGNCC), Nanjing, China, August 12-14, 2016.

[9] Daquan Tang, Yongkang Jiao and Jie Chen, "On Automatic Landing System for carrier plane based on integration of INS, GPS and vision," 2016 IEEE Chinese Guidance, Navigation and Control Conference (CGNCC), Nanjing, China, August 12-14, 2016.

[10] Karl Engelbert Wenzel, Andreas Masselli and Andreas Zell, "Automatic take off, tracking and landing of a miniature UAV on a moving carrier vehicle," Journal of Intelligent & Robotic Systems, vol. 61, no. 1-4, pp. 221-238, 2011.

[11] Daewon Lee, Tyler Ryan and H. Jin. Kim, "Autonomous landing of a VTOL UAV on a moving platform using image-based visual servoing," 2012 IEEE International Conference on Robotics and Automation, Saint Paul, MN, USA, May 14-18, 2012.

[12] Oualid Araar, Nabil Aouf and Ivan Vitanov, "Vision based autonomous landing of multirotor UAV on moving platform," Journal of Intelligent & Robotic Systems, vol. 85, no. 2, pp. 369-384, 2017.

[13] Alexandre Borowczyk, Duc-Tien Nguyen, André Phu-Van Nguyen and Dang Quang Nguyen, "Autonomous landing of a quadcopter on a high-speed ground vehicle," Journal of Guidance Control & Dynamics, vol. 40, no. 9, pp. 1-8, 2017.

[14] Xiao Liang, Guodong Chen, Jiahui Wang and Zheyuan Bi, "An adaptive control system for variable mass quad-rotor UAV involved in rescue missions," International Journal of Simulation: Systems, Science and Technology, vol. 17, no. 29, pp. 22.1-22.7, 2016.

[15] Pedro Castillo Garcia, Rogelio Lozano and Rogelio Lozano, Modeling and control of mini-flying machines. Springer: London, 2005, 142-147.

[16] Fuyang Chen, Feifei Lu, Bin Jiang and Gang Tao, "Adaptive compensation control of the quadrotor helicopter using quantum information technology and disturbance observer," Journal of the Franklin Institute, vol. 351, no. 1, pp. 442-455, 2014.

[17] Olson E, "AprilTag: A robust and flexible visual fiducial system," 2011 IEEE International Conference on Robotics and Automation, Shanghai, China, May 9-13, 2011.

[18] Ksenia Shabalina, Artur Sagitov, Leysan Sabirova, Hongbing Li and Evgeni Magid, "ARTag, AprilTag and CALTag fiducial marker systems: comparison in a presence of partial marker occlusion and rotation," 14th International Conference on Informatics in Control, Automation and Robotics, Madrid, Spain, July 26-28, 2017.

[19] Dawar Khan, Sehat Ullah and Ihsan Rabbi, "Factors affecting the design and tracking of ARToolKit markers," Computer Standards & Interfaces, vol. 41, pp. 56-66, 2015.

[20] Cesare Celozzi, Gianluca Paravati, Andrea Sanna and Fabrizio Lamberti, "A 6-DOF ARTag-based tracking system," IEEE Transactions on Consumer Electronics, vol. 56, no. 1, pp. 203-210, 2010.

[21] Filippo Bergamasco, Andrea Albarelli and Andrea Torsello, "Pi-Tag: a fast image-space marker design based on projective invariants," Machine Vision and Applications, vol. 24, no. 6, pp. 1295-1310, 2013.

[22] Ralph Hartley, Behrooz Kamgar-Parsi and Cody Narber, "Using roads for autonomous air vehicle guidance," IEEE Transactions on Intelligent Transportation Systems, vol. 19, no. 12, pp. 3840-3849, 2018.

[23] He Zhao and Zheyao Wang, "Motion Measurement Using Inertial Sensors, Ultrasonic Sensors, and Magnetometers With Extended Kalman Filter for Data Fusion," IEEE Sensors Journal, vol. 12, no. 5, pp. 943-953, 2012.